Journal of Physics B: Atomic, Molecular and Optical Physics

PAPER

Instability, adiabaticity and controlling effects of external fields for the dark state in a heteronuclear atom–tetramer conversion system

IOP Publishing Journal of Physics B: Atomic, Molecular and Optical Physics
J. Phys. B: At. Mol. Opt. Phys. **47** (2014) 185303 (8pp) doi:10.1088/0953-4075/47/18/185303

Instability, adiabaticity and controlling effects of external fields for the dark state in a heteronuclear atom–tetramer conversion system

Shao-Ying Meng[1], Xi-Hao Chen[1], Shuang-Ning Ning[1], Jia-Mei Wen[1] and Li-Bin Fu[2,3]

[1] Key Laboratory of Optoelectronic Devices and Detection Technology, College of Physics, Liaoning University, Shenyang 110036, People's Republic of China
[2] Science and Technology Computation Physics Laboratory, Institute of Applied Physics and Computational Mathematics, PO Box 8009, Beijing 100088, People's Republic of China
[3] Center for Applied Physics and Technology, Peking University, Beijing 100084, People's Republic of China

E-mail: xi-haochen@163.com and lbfu@iapcm.ac.cn

Received 17 February 2014, revised 31 July 2014
Accepted for publication 5 August 2014
Published 11 September 2014

Abstract
We study the formation of stable heteronuclear tetramers from ultracold atoms via two different paths by generalized Raman adiabatic passage. The dynamical instability and adiabaticity of the dark state are investigated. The regions for the appearance of dynamical instability are analytically obtained and the adiabatic evolution is studied by adiabatic fidelity. Moreover, the effects of the external field parameters on the conversion efficiency are investigated, and a comparison is also drawn between the two different paths.

Keywords: dark state, instability, adiabatic fidelity, ultracold atom-molecule conversion, Raman adiabatic passage

(Some figures may appear in colour only in the online journal)

1. Introduction

The preparation of an ultracold molecular gas has become one of the most interesting areas in the field of ultracold atom-molecule physics in recent years because of its potential application in quantum information [1, 2], in quantum computation [3] and in precision measurement [4, 5]. Currently, two methods are used to create ultracold molecules: direct cooling and indirect cooling. The standard direct laser cooling technique [6–8], as developed for atoms roughly three decades ago, is technically complicated and is difficult for molecules, because of their complex internal energy-level structure. Until recently, this technique was applied to cool SrF [52] and YO [10] to a few millikelvin or less. Other direct cooling strategies include buffer gas cooling [11], Stark or Zeeman deceleration [12–15], velocity filtering [16], sympathetic cooling [17, 18] and Sisyphus cooling [19]. However, these direct cooling approaches have typically been restricted to the millikelvin temperature range. The indirect association techniques from precooled atoms via Feshbach resonances [20–30] (FR) and photoassociation [31–36] (PA) promise access to much lower temperatures. However, these processes either produce molecules exclusively in weakly bound ro-vibrational levels or suffer from low production rates and low state selectively. For the fermionic atoms with FR [25–29], due to the suppression of molecular decay by Pauli blocking, the resulting molecules can be long lived, and some have even been cooled to quantum degeneracy or near-degeneracy.

To produce a quantum gas of molecules in their deeply bound ground state, the stimulated Raman adiabatic passage (STIRAP) technique has been regarded as an effective

method [37–43, 47], taking advantage of the coherent population trapping (CPT) state, or dark state [48–50]. Experimentally, STIRAP has been used to coherently transfer the extremely weakly bound Feshbach molecules to the deeply bound vibrational ground-state diatomic molecules [38–43]. In particular, heteronuclear molecules [41–44] in the vibrational ground state have received a lot of attention, because they possess a strong electric dipole moment, leading to anisotropic, long-range dipole–dipole interactions, which will enable studies of fascinating many-body physics [45, 46]. Very recently, the STIRAP scheme was also used to create the ultracold alkaline-earth-metal $^{84}Sr_2$ molecule [47] from atom pairs on sites of an optical lattice, which can not be formed with the magnetoassociation technique because of the lack of magnetic Feshbach resonances in the nonmagnetic species. With the aid of FR and PA, the generalized Raman adiabactic passage has been proposed to create stable diatomic molecular condensate from an atomic Bose condensate [51], in which a single optical pulse is frequency chirped to compensate for the mean-field shift arising from the particle collisions, so that the CPT condition can be dynamically maintained. This scheme was soon extended to produce the stable homonuclear and heteronuclear triatomic molecules [52–54], and even to convert Bose–Fermi [55] or Fermi–Fermi [56] mixture atoms to their ground state compounded molecules.

As a next step in complexity, the making and probing of ultracold complex molecules has been attracting increasing interest, both in theory and experiment. The first observation of three-body Efimov resonance (ER) molecules [57] (of $^{133}Cs_2$), first predicted in the early 1970 s [58], not only demonstrated the existence of the weakly bound Efimov trimer state but also opened up avenues of exploring intriguing few-body physics. The ER timer molecules were soon observed experimentally in three-component Fermi gases of ^{6}Li [59, 60], in a Bose gas of ^{39}K atoms [61] and even in mixtures of ^{41}K and ^{87}Rb atoms [62]. Not only that, the ER scenario was also extended to four-body systems with identical bosons [63–65]. Experimentally, the tetramer states were recently realized in ultracold gas of cesium atoms [66]. Further extension of the Efimov scenario to five-, six-, seven-, or higher-body cluster states (N-body Borromean) has also been predicted [67–71]. In fact, the Efimov state has a universal characteristic that it does not depend on the details of the pair potential. This makes it possible as an intermediate state transferred to other molecular states and provides important means for assembling ultracold polyatomic molecules. Based on this character, with the help of ER and PA, generalized Raman adiabatic passage has been recently proposed to create tetramers [72, 73], pentamers [74] and even N-body polymer molecules [75]. To obtain higher conversion efficiency, it is crucial to study the stability and adiabaticity of the dark state in these nonlinear atom–molecule conversion systems, as has been widely done in [51, 74–79].

In the present paper, we investigate dynamical instability, adiabaticity and controlling effects of external field parameters for the dark state in the heteronuclear atom–tetramer conversion through generalized Raman adiabatic passage. Here, the heteronuclear tetramers are formed via two paths, i.e., trimers A_3 or A_2B are first created by ER, and then coupled with another atom to a bound tetramer A_3B via PA. We first model the system and derive the coherent atom–molecule dark-state solutions for the two different paths. Then we focus on the dynamical instability analysis of the atom–tetramer dark state via the linear stability theorem, and the unstable parameter regions are obtained analytically. Taking the condensate system of ^{41}K and ^{87}Rb as an example, we further plot the phase diagrams of the instability in the parameter plane. With the help of the adiabatic fidelity, the adiabaticity of the atom–tetramer dark state is also analyzed, and we find that that the first path has better adiabaticity and is more effective than the second one in obtaining higher atom–tetramer conversion efficiency. Moreover, to obtain high atom–tetramer conversion efficiency by choosing suitable parameter values, we also discuss the effects of the single-photon detuning, and the strength and width of the Rabi pulse on the conversion efficiency.

The paper is organized as follows. In section 2, we model the systems and derive the CPT state solution. In section 3, we investigate the dynamical instability of the atom–tetramer dark state, In section 4, we study the adiabatic fidelity and the controlling effects of the external field parameters on the CPT state. In section 5, our conclusion is presented.

2. Model and CPT state solution

With the help of ER and PA, we consider the generalized Raman adiabatic passage to create the ultracold heteronuclear tetramers from Bose atoms via two different reaction paths, which can be denoted by $A_3 + B \rightarrow A_3B$ (AA-path) and $A_2B + A \rightarrow A_3B$ (AB-path). Here, the intermediated trimers A_3 or A_2B are formed by the three-body ER. Then these trimers, along with another atom, are photoassociated to form heteronuclear tetramers. By denoting the atom–trimer coupling strength with λ' and detuning δ, the Rabi frequency of the trimer–tetramer coupling optical field with Ω' and detuning Δ, in the interaction picture, the second quantized Hamiltonian under the rotating frame reads,

$$\hat{H} = \hat{H}_0 + \hat{H}_{int} + \hat{H}_{couple}, \tag{1}$$

where,

$$\hat{H}_0 = -\hbar\left[\delta\hat{\psi}_m{}^\dagger\hat{\psi}_m + \left(\Delta + \delta\right)\hat{\psi}_g{}^\dagger\hat{\psi}_g\right], \tag{2}$$

$$\hat{H}_{int} = -\hbar\sum_{i,j}\chi'_{ij}\hat{\psi}_i{}^\dagger\hat{\psi}_j{}^\dagger\hat{\psi}_j\hat{\psi}_i. \tag{3}$$

For the two paths, the coupling terms are

$$\begin{aligned}\hat{H}^{AA}_{couple} = \; & -\hbar\Big[\lambda'_1\left(\hat{\psi}_m{}^\dagger\hat{\psi}_a\hat{\psi}_a\hat{\psi}_a + H.\,c.\right) \\ & - \Omega'_1\left(\hat{\psi}_g{}^\dagger\hat{\psi}_m\hat{\psi}_b + H.\,c.\right)\Big],\end{aligned} \tag{4}$$

$$\hat{H}^{AB}_{couple} = -\hbar\Big[\lambda_2'\Big(\hat{\psi}_m{}^{\dagger}\hat{\psi}_a\hat{\psi}_a\hat{\psi}_b + H.\,c.\Big) - \Omega_2'\Big(\hat{\psi}_g{}^{\dagger}\hat{\psi}_m\hat{\psi}_a + H.\,c.\Big)\Big]. \quad (5)$$

Here $\hat{\psi}_i$ and $\hat{\psi}_i{}^{\dagger}$ are the annihilation and creation operators for state $|i\rangle$, respectively. The terms proportional to χ_{ij} represent two-body collisions, and the indices $i, j = a, b, m, g$ stand for the atom A, atom B, trimer and tetramer, respectively.

From the Hamiltonian we can easily derive the equations of motion of the unit-scaled operators. Under the mean-field approximation, i.e., $\hat{\psi}_i$ and $\hat{\psi}_i{}^{\dagger}$ are replaced by c-number $\sqrt{n}\psi_i$ and $\sqrt{n}\psi_i^*$, where n is the density of the total particle number. For the AA-path, the set of the mean-field Gross–Pitaevskii (G–P) equations is (with $\hbar = 1$),

$$\begin{aligned} i\dot{\psi}_a &= \omega_a\psi_a - 3\lambda_1\psi_m\psi_a^{*2},\\ i\dot{\psi}_b &= \omega_b\psi_b + \Omega_1\psi_g\psi_m^*,\\ i\dot{\psi}_m &= (\omega_m - i\gamma - \delta)\psi_m - \lambda_1\psi_a^3 + \Omega_1\psi_g\psi_b^*,\\ i\dot{\psi}_g &= \Big(\omega_g - \Delta - \delta\Big)\psi_g + \Omega_1\psi_m\psi_b. \end{aligned} \quad (6)$$

For the AB-path, it becomes

$$\begin{aligned} i\dot{\psi}_a &= \omega_a\psi_a - 2\lambda_2\psi_b^*\psi_b^* + \Omega_2\psi_m^*\psi_g,\\ i\dot{\psi}_b &= \omega_b\psi_b - \lambda_2\psi_m\psi_a^{*2},\\ i\dot{\psi}_m &= (\omega_m - i\gamma - \delta)\psi_m - \lambda_2\psi_a^2\psi_b + \Omega_2\psi_a^*\psi_g,\\ i\dot{\psi}_g &= \Big(\omega_g - \Delta - \delta\Big)\psi_g + \Omega_2\psi_m\psi_a. \end{aligned} \quad (7)$$

In the above two sets of equations (6) and (7), $\omega_i = -2\sum_j\chi_{ij}|\psi_j|^2$, $\chi_{ii} = \chi_{ii}'n$, $\chi_{ij} = \chi_{ij}'n$, $\lambda_i = \lambda_i'\sqrt{n}$, $\Omega_i = \Omega_i'\sqrt{n}$ are the renormalized quantities, and the term proportional to γ is introduced phenomenologically to simulate the loss of intermediate trimers, including the loss process due to collisions. Here, to make our theoretical calculation easy, we have not considered the losses of other channels which also play a crucial role in experiments, but our calculations are still important to guide future efforts.

As in [51–54, 72–75], we now seek the stationary CPT state solutions of equations (6) and (7) with $|\psi_m| = 0$ by introducing the following stationary states:

$$\begin{aligned} \psi_a &= |\psi_a|^0\, e^{i\theta_a}e^{-i\mu_a t},\\ \psi_b &= |\psi_a|^0\, e^{i\theta_b}e^{-i\mu_b t},\\ \psi_m &= |\psi_m|^0\, e^{i\theta_m}e^{-i\mu_m t},\\ \psi_g &= |\psi_g|^0\, e^{i\theta_g}e^{-i\mu_g t}, \end{aligned} \quad (8)$$

where μ_i are the chemical potentials for different species, and $\theta_m = 3\theta_a$, $\mu_m = 3\mu_a$ for the AA-path, while $\theta_m = 2\theta_a + \theta_b$, $\mu_g = 2\mu_a + \mu_b$ for the AB-path. For both the two paths, $\theta_g = 3\theta_a + \theta_b$, $\mu_g = 3\mu_a + \mu_b$, and the normalized condition are the same: $|\psi_a|^2 + |\psi_b|^2 + 3|\psi_m|^2 + 4|\psi_g|^2 = 1$. Substituting equation (8) into equations (6) and (7) and using the conservation conditions of the total particle number for different species of atoms A and B, we can show that the atom–tetramer conversion system supports the following CPT eigenstate,

$$\begin{aligned} |\psi_b^0|^2 &= \frac{-\Omega_i^2 + \Omega_i\sqrt{\Omega_i^2 + k\lambda_i^2}}{2k\lambda_i^2},\\ |\psi_a^0|^2 &= 3|\psi_b^0|^2,\\ |\psi_g^0|^2 &= 1/4 - |\psi_b^0|^2, \end{aligned} \quad (9)$$

where $k = 27(i = 1)$ for the AA-path and $k = 3(i = 2)$ for the AB-path. The chemical potentials and the two-photon resonance conditions are the same for both paths, i.e.,

$$\begin{aligned} \mu_a &= -2\Big(\chi_{aa}|\psi_a^0|^2 + \chi_{ab}|\psi_b^0|^2 + \chi_{ag}|\psi_g^0|^2\Big),\\ \mu_b &= -2\Big(\chi_{ab}|\psi_a^0|^2 + \chi_{bb}|\psi_b^0|^2 + \chi_{bg}|\psi_g^0|^2\Big),\\ \Delta_{AA} &= \Delta_{AB} = -\delta + \Big(6\chi_{ag} + 6\chi_{bg} - 2\chi_{gg}\Big)|\psi_g^0|^2\\ &\quad + \Big(6\chi_{aa} + 2\chi_{ab} - 2\chi_{ag}\Big)|\psi_a^0|^2\\ &\quad + \Big(6\chi_{ab} + 2\chi_{bb} - 2\chi_{bg}\Big)|\psi_b^0|^2. \end{aligned} \quad (10)$$

From equations (9) and (10), we can conclude that, by dynamically maintaining the two-photon resonance condition, population can be concentrated in atomic states and tetramer bound states under the respective limits $\lambda/\Omega \to 0$ and $\lambda/\Omega \to \infty$, which facilitates adiabatic coherent population transfer between atoms and tetramers.

3. Dynamical instability of the CPT state

The existence of the CPT state can not guarantee that it can always be followed adiabatically. In this section, we investigate the stability properties for the heteronuclear atom–tetramer CPT state.

As in [74, 75, 77], we make use of the linear stability analysis through casting the nonlinear Schrödinger equation into an effective classical Hamiltonian and analyzing the eigenvalues of the Hamiltonian–Jacobi matrix obtained by linearizing the equations of motion around the fixed point which corresponds to the CPT state [79, 80]. The instability of the fixed points depends on eigenvalues of the Hamiltonian–Jacobi matrix. Only pure imaginary eigenvalues correspond to the stable fixed points. For this atom–tetramer conversion system, we can obtain the eigenvalues (other than the zero-mode frequency) of the Hamiltonian–Jacobi matrix with an analytic expression,

$$\begin{aligned} \eta_{1,2\pm} &= \pm\frac{i}{\sqrt{2}}\sqrt{B \pm \sqrt{B^2 - C}}\\ B &= \zeta^2 + 2\nu^2 - 2\sigma\eta - 2\alpha\beta\\ C &= 4\Big(\nu^4 - 2\alpha\beta\nu^2 - 2\sigma\eta\nu^2 + \alpha^2\beta^2 + \sigma^2\eta^2 \end{aligned}$$

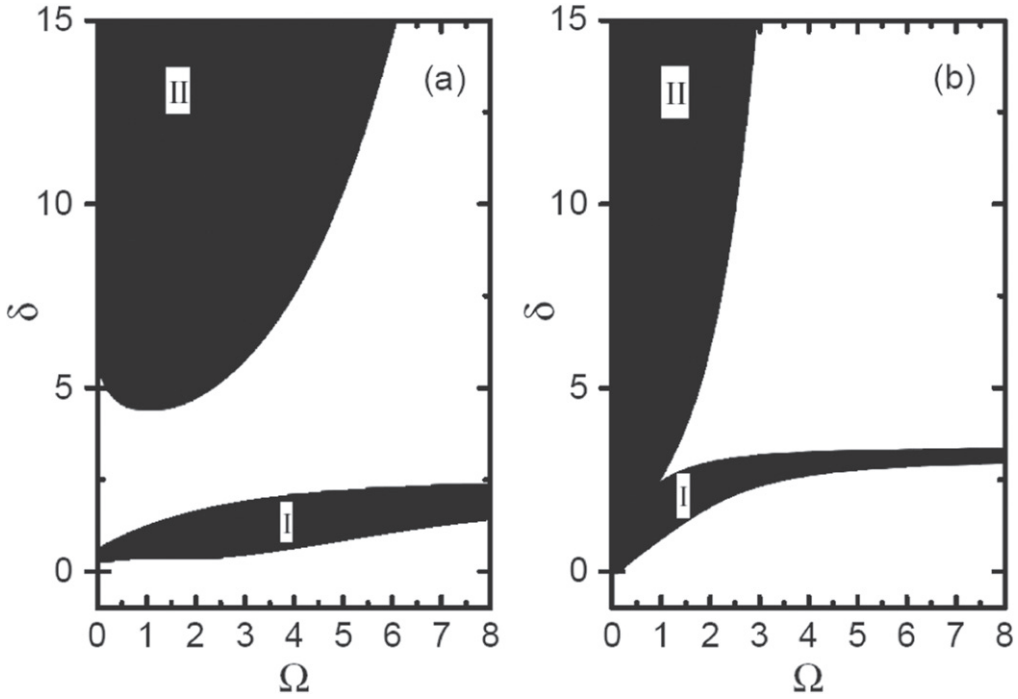

Figure 1. Instability diagrams in δ, Ω space for (*a*) AA-path and (*b*) AB-path, where the black areas correspond to the unstable regions. Here δ and Ω are in units of λ.

$$+ 2\alpha\beta\sigma\eta + 4\chi_{aa}\beta^2\zeta\left|\psi_a^0\right|^2 + 4\chi_{bb}\zeta\eta^2\left|\psi_b^0\right|^2 +4\chi_{gg}\zeta\nu^2\left|\psi_g^0\right|^2 + 8\chi_{ab}\beta\zeta\eta\left|\psi_a^0\right|\left|\psi_b^0\right| + 8\chi_{ag}\beta\zeta\nu\left|\psi_a^0\right|\left|\psi_g^0\right| + 8\chi_{bg}\nu\zeta\eta\left|\psi_b^0\right|\left|\psi_g^0\right|\Big) \quad (11)$$

where

$$\begin{aligned}\alpha^{AA} &= -\beta^{AA} = 3\lambda_1\left|\psi_a^0\right|,\\ \sigma^{AA} &= \eta^{AA} = -\Omega_1\left|\psi_g^0\right|,\\ \nu^{AA} &= \Omega_1\left|\psi_b^0\right|,\\ \zeta^{AA} &= \left(3\chi_{aa} - \chi_{am}\right)\left|\psi_a^0\right|^2 + \left(3\chi_{bb} - \chi_{bm}\right)\left|\psi_b^0\right|^2 + \left(3\chi_{gg} - \chi_{mg}\right)\left|\psi_g^0\right|^2 - \delta \end{aligned} \quad (12)$$

while

$$\begin{aligned}\alpha^{AB} &= 2\lambda_2\left|\psi_a^0\right|\left|\psi_b^0\right| - \Omega_2\left|\psi_g^0\right|,\\ \beta^{AB} &= -2\lambda_2\left|\psi_a^0\right|\left|\psi_b^0\right| - \Omega_2\left|\psi_g^0\right|,\\ \sigma^{AB} &= -\eta^{AB} = \lambda_2\left|\psi_a^0\right|^2,\\ \nu^{AB} &= \Omega_2\left|\psi_a^0\right|,\\ \zeta^{AB} &= \left(4\chi_{aa} + 2\chi_{ab} - 2\chi_{am}\right)\left|\psi_a^0\right|^2 + \left(4\chi_{ab} + 2\chi_{bb}2\chi_{bm}\right)\left|\psi_b^0\right|^2 + \left(4\chi_{ag} + 2\chi_{bg} - 2\chi_{mg}\right)\left|\psi_g^0\right|^2 - \delta \end{aligned} \quad (13)$$

Once $\eta_{1,2\pm}$ become real or complex, the corresponding CPT state is unstable. For the two paths, we find $B > 0$. Hence the unstable regime is given by either $C < 0$ or $C > B^2$. Furthermore, we can see that the instability here strongly depends on the nonlinear collisions. The typical instability diagrams with the parameters of our interest for the AA-path and AB-path are plotted in figures 1(a) and (b), respectively. From these two figures, we see that there are two unstable regions for both paths: region I and region II. Region I is thin along the δ dimension and obtained by setting $C > B^2$; region II occurs at small Ω and corresponds to the unstable region obtained by setting $C < 0$, whose width becomes fat with increasing δ. We can also see that region II emerges when $\delta > 4.4$ or $0.2 < \delta < 2.6$ for the AA-path, while it arises once $\delta > 0$ for the AB-path. Therefore, the adiabatic coherent population transfer from atoms to tetramers can be implemented with a larger parameter range in the δ direction for the AA-path. In order to obtain high conversion efficiency, it is crucial for adiabatic evolution to avoid these unstable regimes when designing the route of adiabatic passage.

In our calculations, we have taken ^{41}K, ^{87}Rb as A and B atoms, respectively. As in [72, 73, 76], the atom–trimer coupling strength is chosen as $\lambda = 4.718 \times 10^4\, s^{-1}$, the condensate density n is $5 \times 10^{20} m^{-3}$, and the collisional parameters are taken as $\chi_{aa} = 0.3214$, $\chi_{bb} = 0.5303$, $\chi_{ab} = 0.8731$, and other collisional parameters are 0.0938, all in units of λ/n.

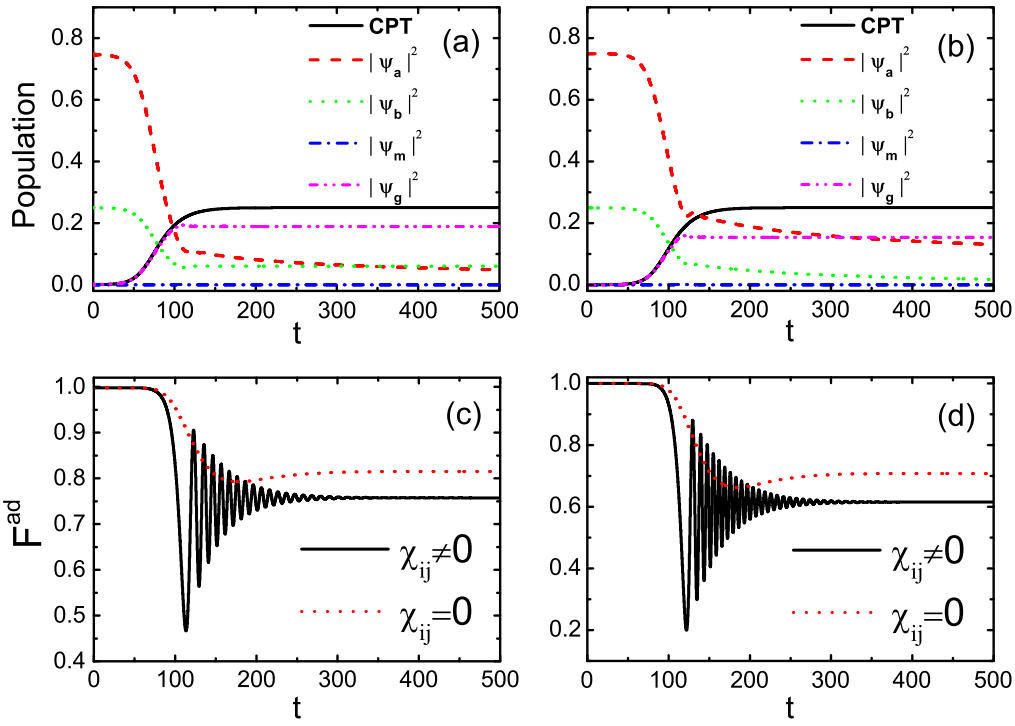

Figure 2. Population (upper) and adiabatic fidelity (lower) as functions of time with $\delta = -3$, $\Omega_0 = 50$, $\tau = 20$, $\gamma = 1$ for the path AA (left) and path AB (right). The adiabatic fidelities without the interparticle interactions are also shown in (*c*) and (*d*), respectively. Here time is in units of λ^{-1} (δ, Ω_0, $\gamma$are in units of λ). Other parameters are defined in section 3.

4. Adiabatic fidelity and controlling effects of external fields for the CPT state

To obtain higher atom–tetramer conversion efficiency, in this section, we investigate the adiabaticity and controlling effects of external fields for the dark state, taking the use of the adiabactic fidelity [74–77], which describes the distance between the CPT solution and the actual evolution of the nonlinear Schödinger equations (6) and (7). From the non-U(1) symmetry of the heteronuclear atom–tetramer conversion system, the adiabatic fidelity of the dark state can be defined as [76, 77]

$$F^{ad} = \left|\left\langle \overline{\psi(t)}\middle|\overline{CPT}\right\rangle\right|^2, \tag{14}$$

where $|\overline{CPT}\rangle$ and $|\overline{\psi(t)}\rangle$ are respectively rescaled wavefunctions of the CPT state and $|\psi(t)\rangle=\left(\psi_a, \psi_b, \psi_m, \psi_g\right)^T$,

$$\left|\overline{\psi(t)}\right\rangle = \left(\frac{\psi_a^3\psi_b}{|\psi_a||\psi_b|}, \frac{\psi_a^3\psi_b}{|\psi_a|^3}, \frac{\sqrt{3}\psi_j\psi_m}{|\psi_j|}, 2\psi_g\right) \tag{15}$$

where $j = b$ for the AA-path and $j = a$ for the AB-path. If the system can adiabatically evolve along the CPT state, then the value of the adiabatic fidelity should be close to 1. In our calculations, the Rabi frequency is modulated as

$$\Omega = \Omega_0 \,\mathrm{sech}\,(t/\tau) \tag{16}$$

where Ω_0 and τ are respectively the strength and width of the pulse. In order to describe the actual loss of intermediate trimers in the process, we set the decay rate $\gamma = 1$, which is given in units of λ.

Figure 2 shows the population and the adiabatic fidelity of the CPT state as functions of time for the AA-path (left) and AB-path (right), where the parameter δ is chosen in the stable regions. As can be seen in figures 2(c) and (d), the adiabatic fidelity is about 1 at the initial time, but begins to decrease at some later time, then diminishes to the minimal values 0.46 and 0.2 at time 113 and 122 for the AA-path and AB-path, respectively. This implies the system initially evolves adiabatically along the CPT state, then deviates from the CPT state, as is shown in the population dynamics in figures 2(a) and (b). Although the fidelity fluctuates later on, the final values are no more than 0.75 and 0.61. In comparison with the results in path AA and path AB, we conclude that the adiabaticity of the system for the AA-path is better than the AB-path. Therefore, the former path can result in a higher yield of tetramers than the second one, as is shown in figures 2(a) and (b). Moreover, once the interparticle interactions are considered, the adiabatic fidelity is poor. Therefore, the nonlinear collisions suppress the conversion from atoms to tetramers. The above conclusions are still right for many other sets of parameters provided that the dynamical stability is assured. This will be shown in the following discussions.

The dependence of the final adiabatic fidelity F_f^{ad} which can be used to describe the conversion efficiency on the external field parameters for the two paths is shown in figure 3. From this figure, we see that the stable creation of tetramers is always possible for $\delta < 0$ no matter whether the nonlinear collisions are included. However, once the interparticle interactions are included, the conversion efficiency is

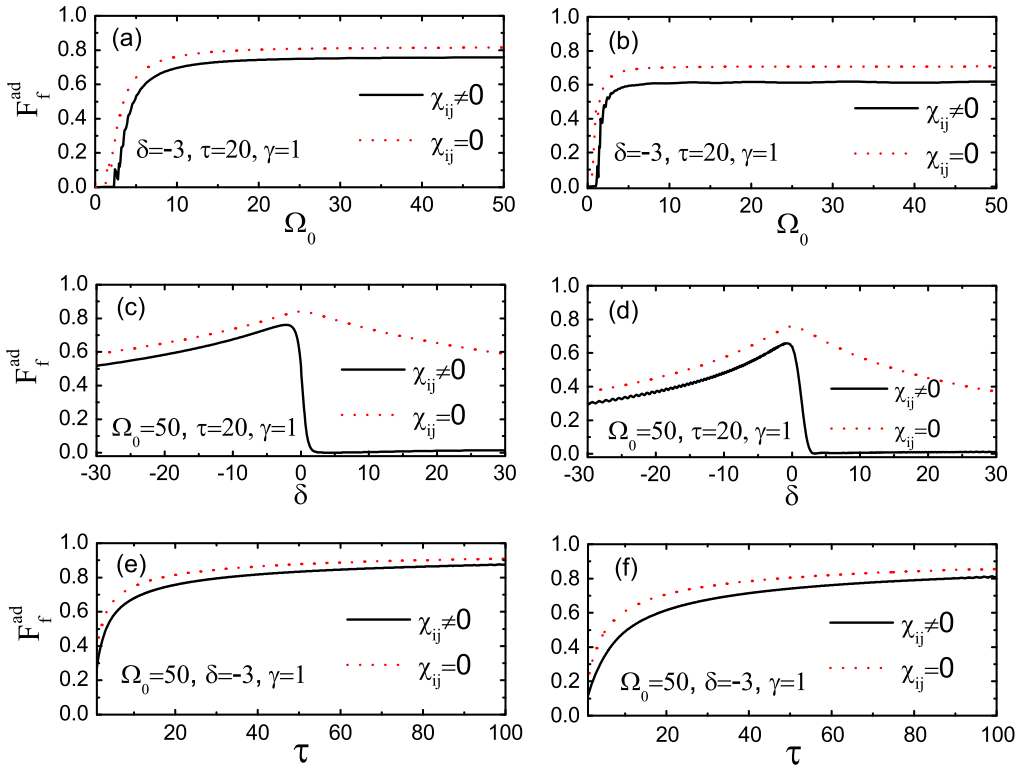

Figure 3. Effects of the external field parameters on the conversion efficiency for the AA-path (left) and AB-path (right). The adiabatic fidelity vs (a), (b) the detuning δ, (c), (d) the Rabi pulse strength Ω_0, (e), (f) the pulse width τ. Time is in units of λ^{-1}, other parameters are in units of λ and are defined in section 3.

near to zero for $\delta > 0$. Moreover, as the Rabi pulse amplitude Ω_0 and width τ increase, the conversion efficiency first increases quickly, then reaches a steady optimal value which is close to 1. After comparing the results with and without the two-body interactions, we find the two-body interactions suppress the conversion of tetramers. It is clear that we can improve the conversion efficiency by choosing the optimal external field parameters δ, Ω_0, and τ. Moreover, we can also find that the AA-path is more favorable than the AB-path to obtain high conversion efficiency. For example, comparing figures 3(a) and (b), it is found that the conversion efficiency for the AA-path is always higher than the AB-path once $\Omega_0 > 7$ with the same external parameters, no matter whether the nonlinear collisions are considered. If we compare figures 3(c) and (d) (or figures 3(e) and (f)), we can obtain the same conclusion on the premise that stability of the CPT state is guaranteed. Therefore, the AA-path is more favorable than the AB-path.

It should also be noted here that the parameter γ is chosen as a fixed value of 1. In fact, once γ becomes larger, its negative influence on the atom–tetramer conversion efficiency will become more significant, which has not been shown here.

5. Conclusion

In summary, we have investigated the heteronuclear molecular tetramer conversion problem via a generalized Raman adiabatic passage through two different paths, AA and AB. The CPT state solution has been derived, and the dynamical instability and adiabaticity of the atom–tetramer dark state have been studied by linear stability analysis and adiabatic fidelity, respectively. For the two paths, the unstable parameter regions are given analytically. And taking the ^{41}K-^{87}Rb mixture condensate system as an example, we give the unstable regions numerically. Moreover, the effects of the external field parameters on the conversion efficiency are studied by the adiabatic fidelity. We find that one can improve the conversion efficiency by optimizing the single-photon detuning, the strength and the width of the Rabi pulse. In addition, our calculation suggests that, in most cases, the adiabaticity of the dark state in the AA-path is better than that in the AB-path, hence the first path is more effective than the second one in obtaining higher atom–tetramer conversion efficiency.

Acknowledgments

This work is supported by the National Natural Science Foundation of China (grants no. 11005055, 11075020, 11204117, 11305120), the National Fundamental Research Programme of China under grant no. 2011CB921503, and the Higher School Excellent Researcher Award Program from the Educational Department of Liaoning Province of China (grant no. LJQ2011005).

References

[1] André A, DeMille D, Doyle J M, Lukin M D, Maxwell S E, Rabl P, Schoelkopf R J and Zoller P 2006 *Nature Phys.* **2** 636
[2] Schuster D, Bishop L, Chuang I, DeMille D and Schoelkopf R 2011 *Phys. Rev.* A **83** 012311
[3] DeMille D 2002 *Phys. Rev. Lett.* **88** 067901
[4] Hudson E R, Lewandowski H J, Sawyer B C and Ye J 2006 *Phys. Rev. Lett.* **96** 143004
[5] Chin C, Flambaum V V and Kozlov M G 2009 *New J. Phys.* **11** 055048
[6] Chu S 1998 *Rev. Mod. Phys.* **70** 685
[7] Cohen-Tannoudji C N 1998 *Rev. Mod. Phys.* **70** 707
[8] Phillips W D 1998 *Rev. Mod. Phys.* **70** 721
[9] Shuman E S, Barry J F and Demille D 2010 *Nature* **467** 820
[10] Hummon M T, Yeo M, Stuhl B K, Collopy A L, Xia Y and Ye J 2012 *Phys. Rev. Lett.* **110** 143001
[11] Weinstein J D, deCarvalho R, Guillet T, Friedrich B and Doyle J M 1998 *Nature* **395** 148
[12] Sawyer B C, Lev B L, Hudson E R, Stuhl B K, Lara M, Bohn J L and Ye J 2007 *Phys. Rev. Lett.* **98** 253002
[13] van de Meerakker S Y T, Bethlem H L and Meijer G 2008 *Nature Phys.* **4** 595
[14] Elioff M S, Valentini J J and Chandler D W 2003 *Science* **302** 1940
[15] Vanhaecke N, Meier U, Andrist M, Meier B H and Merkt F 2007 *Phys. Rev.* A **75** 031402
[16] Rangwala S A, Junglen T, Rieger T, Pinkse P W and Rempe G 2003 *Phys. Rev.* A **67** 043406
[17] Doyle J, Friedrich B, Krems R V and Masnou-Seeuws F 2004 *Eur. Phys. J.* D **31** 149
[18] Rellergert Wade G, Sullivan Scott T, Schowalter S J, Kotochigova S, Chen K and Hudson E R 2013 *Nature* **495** 490
[19] Zeppenfeld M, Englert B G U, Glöckner R, Prehn A, Mielenz M, Sommer C, van Buuren L D, Motsch M and Rempe G 2012 *Nature* **491** 570
[20] Inouye S, Andrews M R, Stenger J, Miesner H J, Stamper-Kurn D M and Ketterle W 1998 *Nature* **151** 392
[21] Donley E A, Claussen N R, Thompson S T and Wieman C E 2002 *Nature* **417** 529
[22] Chin C, Kerman A J, Vuletić V and Chu S 2003 *Phys. Rev. Lett.* **90** 033201
[23] Xu K, Mukaiyama T, Abo-Shaeer J R, Chin J K, Miller D E and Ketterle W 2003 *Phys. Rev. Lett.* **91** 210402
[24] Herbig J, Kraemer T, Mark M, Weber T, Chin C, Nägerl H-C and Grimm R 2003 *Science* **301** 1510
[25] Regal C A, Ticknor C, Bohn J L and Jin D S 2003 *Nature* **424** 47
[26] Greiner M, Regal C and Jin D S 2003 *Nature* **426** 537
[27] Jochim S, Bartenstein M, Altmeyer A, Hendl G, Riedl S, Chin C, Hecker Denschlag J and Grimm R 2003 *Science* **302** 2101
[28] Zwierlein M W, Stan C A, Schunck C H, Raupach S M F, Gupta S, Hadzibabic Z and Ketterle W 2003 *Phys. Rev. Lett.* **91** 250401
[29] Bourdel T, Khaykovich L, Cubizolles J, Zhang J, Chevy F, Teichmann M, Tarruell L, Kokkelmans S J J M F and Salomon C 2004 *Phys. Rev. Lett.* **93** 050401
[30] Köhler T, Góral K and Julienne P S 2006 *Rev. Mod. Phys.* **78** 1311 and reference therein
[31] Viteau M, Chotia A, Allegrini M, Bouloufa N, Dulieu O, Comparat D and Pillet P 2008 *Science* **321** 232
[32] Kerman A J, Sage J M, Sainis S, Bergeman T and DeMille D 2004 *Phys. Rev. Lett.* **92** 153001
[33] Mancini M W, Telles G D, Caires A R L, Bagnato V S and Marcassa L G 2004 *Phys. Rev. Lett.* **92** 133203
[34] Wang D, Qi J, Stone M F, Nikolayeva O, Wang H, Hattaway B, Gensemer S D, Gould P L, Eyler E E and Stwalley W C 2004 *Phys. Rev. Lett.* **93** 243005
[35] Sage J M, Sainis S, Bergeman T and DeMille D 2005 *Phys. Rev. Lett.* **94** 203001
[36] Deiglmayr J, Grochola A, Repp M, Mötlbauer K, Glück C, Lange J, Dulieu O, Wester R and Weidemüller M 2008 *Phys. Rev. Lett.* **101** 133004
[37] Winkler K, Thalhammer G, Theis M, Ritsch H, Grimm R and Denschlag J H 2005 *Phys. Rev. Lett.* **95** 063202
[38] Winkler K, Lang F, Thalhammer G, v d Straten P, Grimm R and Denschlag J H 2007 *Phys. Rev. Lett.* **98** 043201
[39] Lang F, Winkler K, Strauss C, Grimm R and Hecker Denschlag J 2008 *Phys. Rev. Lett.* **101** 133005
[40] Danzl J G, Haller E, Gustavsson M, Mark M J, Hart R, Bouloufa N, Dulieu O, Ritsch H and Nägerl H-C 2008 *Science* **321** 1062
[41] Ni K-K, Ospelkaus S, de Miranda M H G, Pe'er A, Neyenhuis B, Zirbel J J, Kotochigova S, Julienne P S, Jin D S and Ye J 2008 *Science* **322** 231
[42] Ospelkaus S, Pe'er A, Ni K-K, Zirbel J J, Neyenhuis B, Kotochigova S, Julienne P S, Ye J and Jin D S 2008 *Nature Physics* **4** 622
[43] Spiegelhalder F M, Trenkwalder A, Naik D, Kerner G, Wille E, Hendl G, Schreck F and Grimm R 2010 *Phys. Rev.* A **81** 043637
[44] Takekoshi T, Reichsöllner L , Schindewolf A, Hutson J M, Le Sueur C R, Dulieu O, Ferlaino F, Grimm R, and Nägerl H-C, preprint at: arXiv:1405.6037
[45] Büchler H P, Demler E, Lukin M, Micheli A, Prokof'ev N, Pupillo G and Zoller P 2007 *Phys. Rev. Lett.* **98** 060404
[46] Pupillo G, Micheli A, Büchler H P and Zoller P 2007 *Phys. Rev.* A **76** 043604
[47] Stellmer S, Pasquiou B, Grimm R and Schreck F 2012 *Phys. Rev. Lett.* **109** 115302
[48] Mackie M, Kowalski R and Javanainen J 2000 *Phys. Rev. Lett.* **84** 3803
[49] Drummond P D, Kheruntsyan K V, Heinzen D J and Wynar R H 2002 *Phys. Rev.* A **65** 063619
[50] Bergmann K, Theuer H and Shore B W 1998 *Rev. Mod. Phys.* **70** 1003
[51] Ling H Y, Pu H and Seaman B 2004 *Phys. Rev. Lett.* **93** 250403
[52] Jing H, Cheng J and Meystre P 2007 *Phys. Rev. Lett.* **99** 133002
[53] Jing H, Cheng J and Meystre P 2008 *Phys. Rev.* A **77** 043614
[54] Jing H, Zheng F, Jiang Y and Geng Z 2008 *Phys. Rev.* A **78** 033617
[55] Lu L H and Li Y Q 2007 *Phys. Rev.* A **76** 053608
[56] Lu L H and Li Y Q 2008 *Phys. Rev.* A **77** 053611
[57] Kraemer T *et al* 2006 *Nature* **440** 315
[58] Efimov V 1970 *Phys. Lett.* **33B** 563
[59] Ottenstein T B, Lompe T, Kohnen M, Wenz A N and Jochim S 2008 *Phys. Rev. Lett.* **101** 203202
[60] Huckans J H, Williams J R, Hazlett E L, Stites R W and O'Hara K M 2009 *Phys. Rev. Lett.* **102** 165302
[61] Zaccanti M, Deissler B, D'Errico C, Fattori M, Jona-Lasinio M, Muller S, Roati G, Inguscio M and Modugno G 2009 *Nature Phys.* **5** 586
[62] Barontini G, Weber C, Rabatti F, Catani J, Thalhammer G, Inguscio M and Minardi F 2009 *Phys. Rev. Lett.* **103** 043201
[63] von Stecher J, D'Incao J P and Greene C H 2009 *Nature Phys.* **5** 417
[64] Pollack S E, Dries D and Hulet R G 2009 *Science* **326** 1683
[65] Hadizadeh M R, Yamashita M T, Tomio L, Delfino A and Frederico T 2011 *Phys. Rev. Lett.* **107** 135304
[66] Ferlaino F, Knoop S, Berninger M, Harm W, D'Incao J P, Nägerl H-C and Grimm R 2009 *Phys. Rev. Lett.* **102** 140401

[67] von Stecher J 2010 *J. Phys.* B **43** 101002
von Stecher J 2011 *Phys. Rev. Lett.* **107** 200402
[68] Thoersen M, Fedorov D V and Jensen A S 2008 *Europhys. Lett.* **83** 30012
[69] Hanna G J and Blume D 2006 *Phys. Rev.* A **74** 063604
[70] Yamashita M T, Fedorov D V and Jensen A S 2010 *Phys. Rev.* A **81** 063607
[71] Zenesini A, Huang B, Berninger M, Besler S, Nägerl H-C, Ferlaino F, Grimm R, Greene C H and von Stecher J 2013 *New J. Phys.* **15** 043040
[72] Jing H and Jiang Y 2008 *Phys. Rev.* A **77** 65601
[73] Li G Q and Peng P 2011 *Phys. Rev.* A **83** 043605
[74] Dou F Q, Li S C, hui Cao and Fu L B 2012 *Phys. Rev.* A **85** 023629
[75] Dou F Q, Fu L B and Liu J 2013 *Phys. Rev.* A **87** 043631
[76] Meng S Y, Fu L B and Liu J 2008 *Phys. Rev.* A **78** 053410
[77] Meng S Y, Fu L B and Liu J 2009 *Phys. Rev.* A **79** 063415
[78] Pu H, Maenner P, Zhang W P and Ling H Y 2007 *Phys. Rev. Lett.* **98** 050406
[79] Itin A P and Watanabe S 2007 *Phys. Rev. Lett.* **99** 223903
[80] Liu J, Wu B and Niu Q 2003 *Phys. Rev. Lett.* **90** 170404